Journal of Magnetism and Magnetic Materials 324 (2012) 2977–2982

Contents lists available at SciVerse ScienceDirect

Journal of Magnetism and Magnetic Materials

journal homepage: www.elsevier.com/locate/jmmm

Magnetic structure of the La_3NiGe_2-type Tb_3NiGe_2 and Mn_5Si_3-type $Tb_5Ni_xGe_{3-x}$ ($x=0$ and 0.3)

A.V. Morozkin [a,*], Jinlei Yao [b], Y. Mozharivskyj [b], O. Isnard [c]

[a] Department of Chemistry, Moscow State University, Leninskie Gory, House 1, Building 3, Moscow GSP-2 119992, Russia
[b] Department of Chemistry and Chemical Biology, McMaster University, 1280 Main Street West, Hamilton, Ontario, Canada L8S 4M1
[c] Institut Néel, CNRS—Université Joseph Fourier, Departement MCMF, 25 rue des Martyrs, BP 166, 38042 Grenoble cedex 9, France

ARTICLE INFO

Article history:
Received 25 October 2011
Received in revised form
23 March 2012
Available online 15 May 2012

Keywords:
Rare earth intermetallics
Neutron diffraction
Magnetic structure

ABSTRACT

We present a neutron powder diffraction investigation of the magnetic structure of La_3NiGe_2-type Tb_3NiGe_2 and Mn_5Si_3-type $Tb_5Ni_xGe_{3-x}$ ($x=0$, 0.3) compounds. It is found that below ~135 K Tb_3NiGe_2 exhibits a commensurate *b*-collinear ferrimagnetic ordering with $\mathbf{C}_{2h'}=\{\mathbf{1}, \mathbf{m}_z, 1' \times \mathbf{2}_z, 1' \times \mathbf{1}\}$ magnetic point group. The Mn_5Si_3-type Tb_5Ge_3 and $Tb_5Ni_{0.3}Ge_{2.7}$ compounds are found to present a flat spiral type antiferromagnetic ordering at 85 and $\geq$89 K, respectively. The Ni for Ge substitution is found to decrease the flat spiral ordered magnetic unit cell from $a \times a \times 40c$ of Tb_5Ge_3 (below 40 K) down to $a \times a \times 5c$ for $Tb_5Ni_{0.3}Ge_{2.7}$ (below ~10 K).

1. Introduction

The Tb_3NiGe_2 compound crystallizes in the La_3NiGe_2-type (space group *Pnma*) structure. The La_3NiGe_2 structure is a member of the family of two-layer orthorhombic structures with *Pnma* symmetry and a set of special 4*c* sites (*x*, 1/4, *z*) derived from the hexagonal Mg structure [1]. The Mn_5Si_3-type Tb_5Ge_3 compound (space group $P6_3/mcm$) has been shown to present a flat spiral *ab*-plane antiferromagnetic ordering with Tb magnetic moment of 6*g* site equaling that of 4*d* site at 2 K ($M_{Tb6g,\ 4d}=8.9\ \mu_B$ at 2 K) and wave vector decreasing from $K=[0, 0, 1/2]$ around $T_N=85$ K down to $K=[0, 0, \pm\ 0.4616]$ at 2 K [1,2].

This work aims to understand the nature of the magnetic ordering in Tb_3NiGe_2 via neutron diffraction study of the two-phase sample that contains the La_3NiGe_2-type Tb_3NiGe_2 and Mn_5Si_3-type $Tb_5Ni_{0.3}Ge_{2.7}$ compounds. To solve this task the magnetic structure of Tb_5Ge_3 was also re-investigated here.

2. Experimental details

The Tb_3NiGe_2 and Tb_5Ge_3 samples were prepared by arc-melting weighed amounts of terbium (99.9 wt%), nickel (99.95 wt%) and germanium (99.99 wt%). The samples were annealed at 1070 K for 150 h in an argon atmosphere and quenched in ice-cold water.

The quality of the samples was evaluated using powder X-ray diffraction (XRD) and X-ray spectral microprobe analyses. The XRD data were obtained on a DRON-3.0 diffractometer (Cu Kα radiation, $2\Theta=10$–80°, step 0.05°, 3 s per step) at room temperature. The unit cell data were derived using the Rietan-program [3] in the isotropic approximation. A 'Camebax' microanalyzer was employed to perform microprobe X-ray spectral analysis of the samples ((15 kV, 3×10^{-8} A), *K*-, *L*- and *M*-lines, $2\times2\ \mu m^2$).

The dc magnetization was measured on a commercial SQUID magnetometer (Quantum Design) in the temperature range 5–300 K in an applied field of 0.01 T (100 Oe).

The neutron diffraction experiments were carried out on a D1B powder diffractometer [4] ($\lambda=0.252$ nm at the Institute Laue-Langevin, Grenoble, France). The neutron diffraction patterns were identified and calculated using the FULLPROF-program in terms of traditional crystallographic approach [5].

3. Results and discussion

3.1. Sample composition

The quantitative microprobe X-ray analysis of samples led to the identification of the following phases in the 'Tb_3NiGe_2' sample: $Tb_{50}Ni_{17}Ge_{33}$ and $Tb_{62}Ni_4Ge_{34}$, whereas 'Tb_5Ge_3' is single-phase ($Tb_{62}Ge_{38}$) (Fig. 1). The 'Tb_3NiGe_2' sample contains 0.90 mass fraction of the La_3NiGe_2-type Tb_3NiGe_2 and 0.10 mass fraction of the Mn_5Si_3-type $Tb_5Ni_xGe_{3-x}$ revealed by the Rietveld refinements on the XRD data (Table 1). The estimation of the

* Corresponding author.
E-mail address: morozkin@general.chem.msu.ru (A.V. Morozkin).

0304-8853/$ - see front matter © 2012 Elsevier B.V. All rights reserved.
http://dx.doi.org/10.1016/j.jmmm.2012.04.023

quantity of each phase in the 'Tb_3NiGe_2' has been done by the Rietveld refinements on the XRD data.

The atomic sites of the Mn_5Ge_3-type Tb_5Ge_3, $Tb_5Ni_xGe_{3-x}$ and the La_3NiGe_2-type Tb_3NiGe_2 are given in Table 2. The Mn_5Si_3-type phase has been subsequently included in the refinements of the powder neutron diffraction data of the 'Tb_3NiGe_2' sample.

The results of dc magnetization and inverse susceptibility measurements of polycrystalline sample 'Tb_3NiGe_2' are given in Fig. 2. The paramagnetic susceptibility follows the Curie–Weiss law in the temperature range 150–350 K. The fit yields a positive paramagnetic Curie temperature $\Theta_p = 122.4$ K, suggesting dominant ferromagnetic interactions. The effective paramagnetic moments per formula unit M_{eff}/fu of 17.21 μ_B gave an effective magnetic moment of the Ni atom as 3.57 μ_B assuming terbium takes the theoretical moment 9.72 μ_B [6] (Fig. 2a).

According to the magnetization measurement Tb_3NiGe_2 undergoes a ferromagnetic-type transition at 128 K (Fig. 2b).

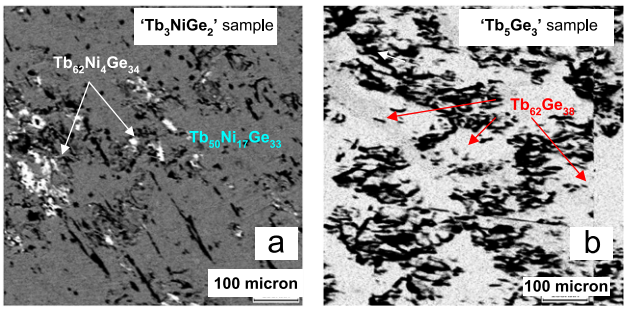

Fig. 1. SEM photo of (a) 'Tb_3NiGe_2 and (b) 'Tb_5Ge_3' samples. Compositions of the different phases are given in the figure.

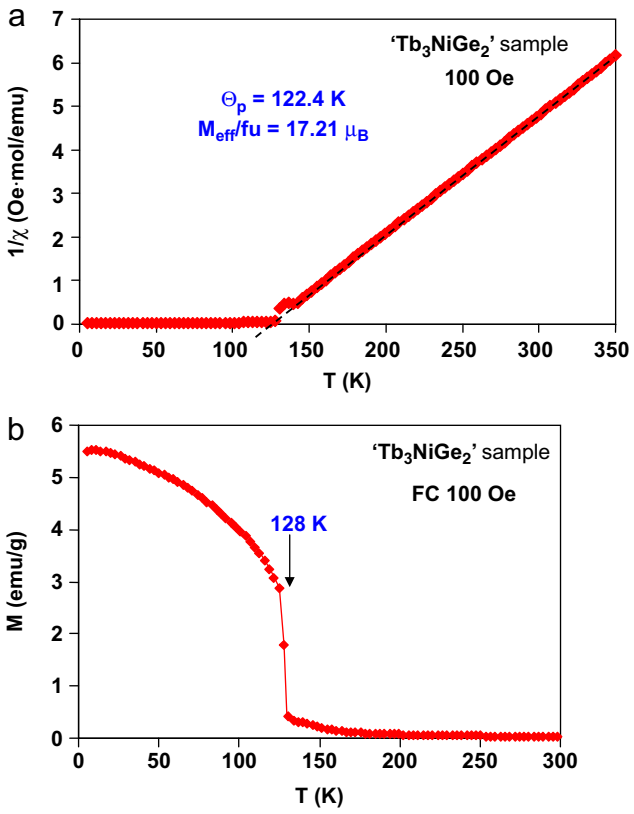

Fig. 2. Inverse magnetic susceptibility (a) and magnetization (b) vs. temperature of the 'Tb_3NiGe_2' sample.

Table 1
The composition of the 'Tb_5Ge_3' and 'Tb_3NiGe_2' samples and cell parameters of compounds at room temperature (X-ray spectral and X-ray powder data).

Sample	Mass fraction	Compound	Structure	Space group	*a* (nm)	*b* (nm)	*c* (nm)	R_F (%)
'Tb_5Ge_3'	1.00	Tb_5Ge_3	Mn_5Si_3	*P6₃/mcm*	0.84956(6)		0.63861(4)	4.1
'Tb_3NiGe_2'	0.90	Tb_3NiGe_2	La_3NiGe_2	*Pnma*	1.1403(1)	0.41793(4)	1.1248(1)	2.5
	0.10	$Tb_5Ni_{0.3}Ge_{2.7}$	Mn_5Si_3	*P6₃/mcm*	0.8472(3)		0.6348(2)	2.3

Table 2
Atomic sites in the La_3NiGe_2-type Tb_3NiGe_2 and Mn_5Si_3-type Tb_5Ge_3 and $Tb_5Ni_{0.3}Ge_{2.7}$ (X-ray powder data at room temperature) and atomic position of terbium sublattice in the Mn_5Si_3-type terbium sublattice in term of *P1* space group.

Compound	Atom	Site	x/a	y/b	z/c
Tb_3NiGe_2	Tb1	*4c*	0.3812(6)	1/4	0.4417(6)
	Tb2	4c	0.0541(6)	1/4	0.3750(6)
	Tb3	4c	0.2176(7)	1/4	0.6956(6)
	Ni	4c	0.125(2)	1/4	0.125(2)
	Ge1	4c	0.481(1)	1/4	0.690(1)
	Ge2	4c	0.305(1)	1/4	−0.002(1)
Tb_5Ge_3	Tb1	6g	0.2407(4)	0	1/4
	Tb2	4d	1/3	2/3	0
	Ge	6g	0.6019(7)	0	1/4
$Tb_5Ni_{0.3}Ge_{2.7}$	Tb_{6g}	6g	0.232(2)	0	1/4
	Tb_{4d}	4d	1/3	2/3	0
	$Ni_{0.1}Ge_{0.9}$	6g	0.597(3)	0	1/4
Terbium sublattice of Tb_5Ge_3 and $Tb_5Ni_xGe_{3-x}$ in term of *P1* space group	Tb^1_{6g}	*1*	X_{Tb1}	0	1/4
	Tb^2_{6g}	*1*	0	X_{Tb1}	1/4
	Tb^3_{6g}	*1*	$-X_{Tb1}$	$-X_{Tb1}$	1/4
	Tb^4_{6g}	*1*	$-X_{Tb1}$	0	3/4
	Tb^5_{6g}	*1*	0	$-X_{Tb1}$	3/4
	Tb^6_{6g}	*1*	X_{Tb1}	X_{Tb1}	3/4
	Tb^1_{4d}	*1*	1/3	2/3	0
	Tb^2_{4d}	*1*	2/3	1/3	0
	Tb^3_{4d}	*1*	1/3	2/3	1/2
	Tb^4_{4d}	*1*	2/3	1/3	1/2

3.2. Magnetic structure of Mn_5Si_3-type Tb_5Ge_3 and admixture $Tb_5Ni_{0.3}Ge_{2.7}$

The neutron diffraction patterns of Tb_5Ge_3 and the 'Tb_3NiGe_2' sample obtained at different temperatures are given in Figs. 3 and 4. An analysis of the low temperature patterns reveals that the magnetic reflections of Tb_5Ge_3 correspond to a unit cell with propagation vectors $K=[0, 0, \pm K_c]$ and flat spiral antiferromagnetic ordering, confirming the results reported in Ref. [2]. Thermal variation of the Tb magnetic moments at the 6*g* and 4*d* sites is given in Fig. 5. Down to 17 K the terbium magnetic moment at the 6*g* site is smaller than at the 4*d* site position. Below 17 K these magnetic moments are the same and reach the value 7.8 μ_B/Tb, a value significantly smaller than the 9 μ_B expected for free ion Tb^{3+} [6]. The thermal variation of the propagation vector K_c indicates that between 85 and 77 K the magnetic unit cell is $a\times a\times 2c$ and below 40 K it is $a\times a\times 40c$. Between 77 and 40 K the $a\times a\times 2c$ magnetic unit cell transforms continuously to the $a\times a\times 40c$ one (Fig. 5c).

For $Tb_5Ni_{0.3}Ge_{2.7}$ the low-angle incommensurate magnetic reflection indicates the antiferromagnetic ordering at $\geq$89 K. An analysis

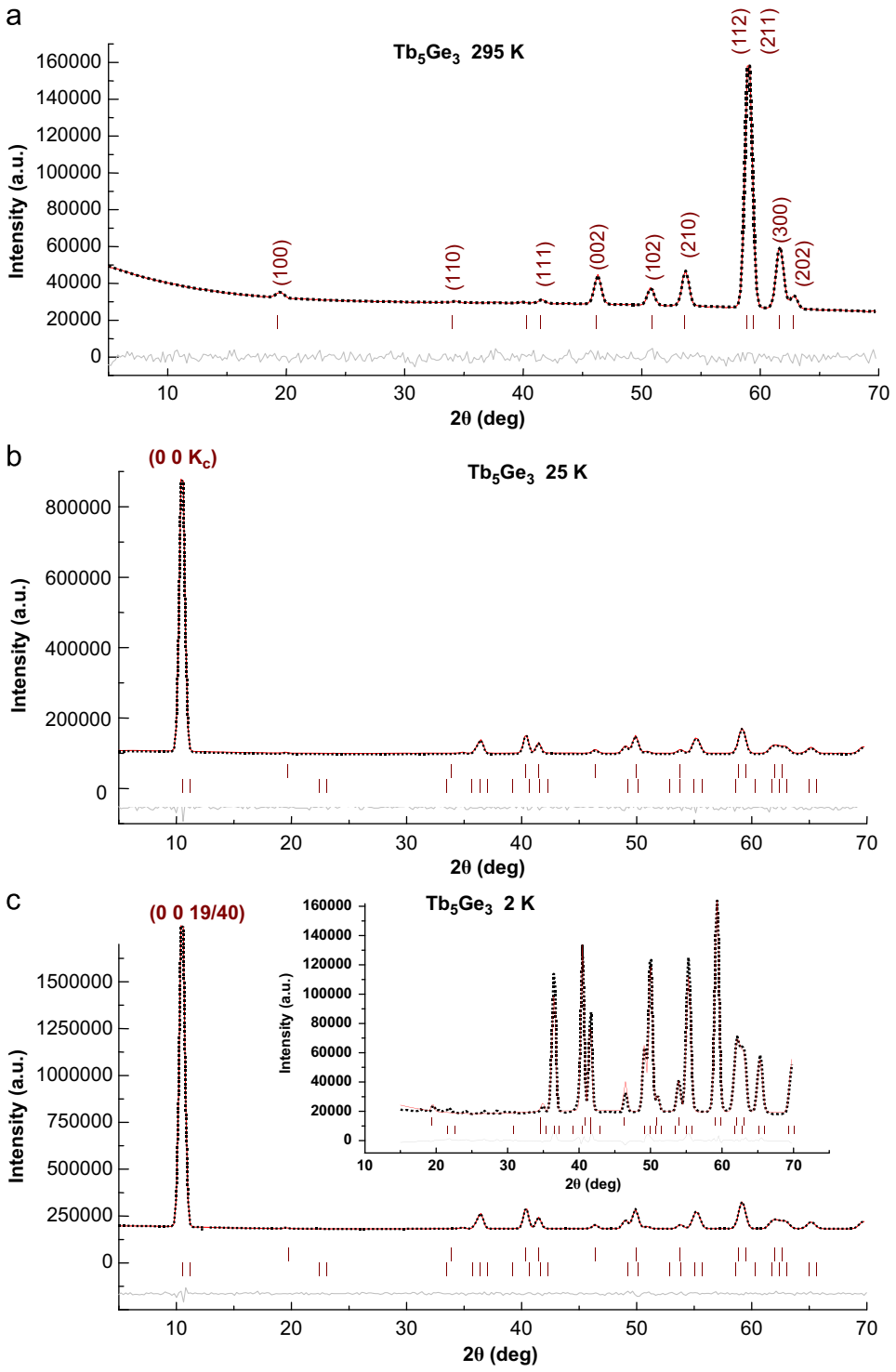

Fig. 3. Neutron diffraction patterns of the 'Tb_5Ge_3' sample (a) at 295 K (paramagnetic state), (b) at 25 K and (c) at 2 K (antiferromagnetic state) (λ=0.252 nm).

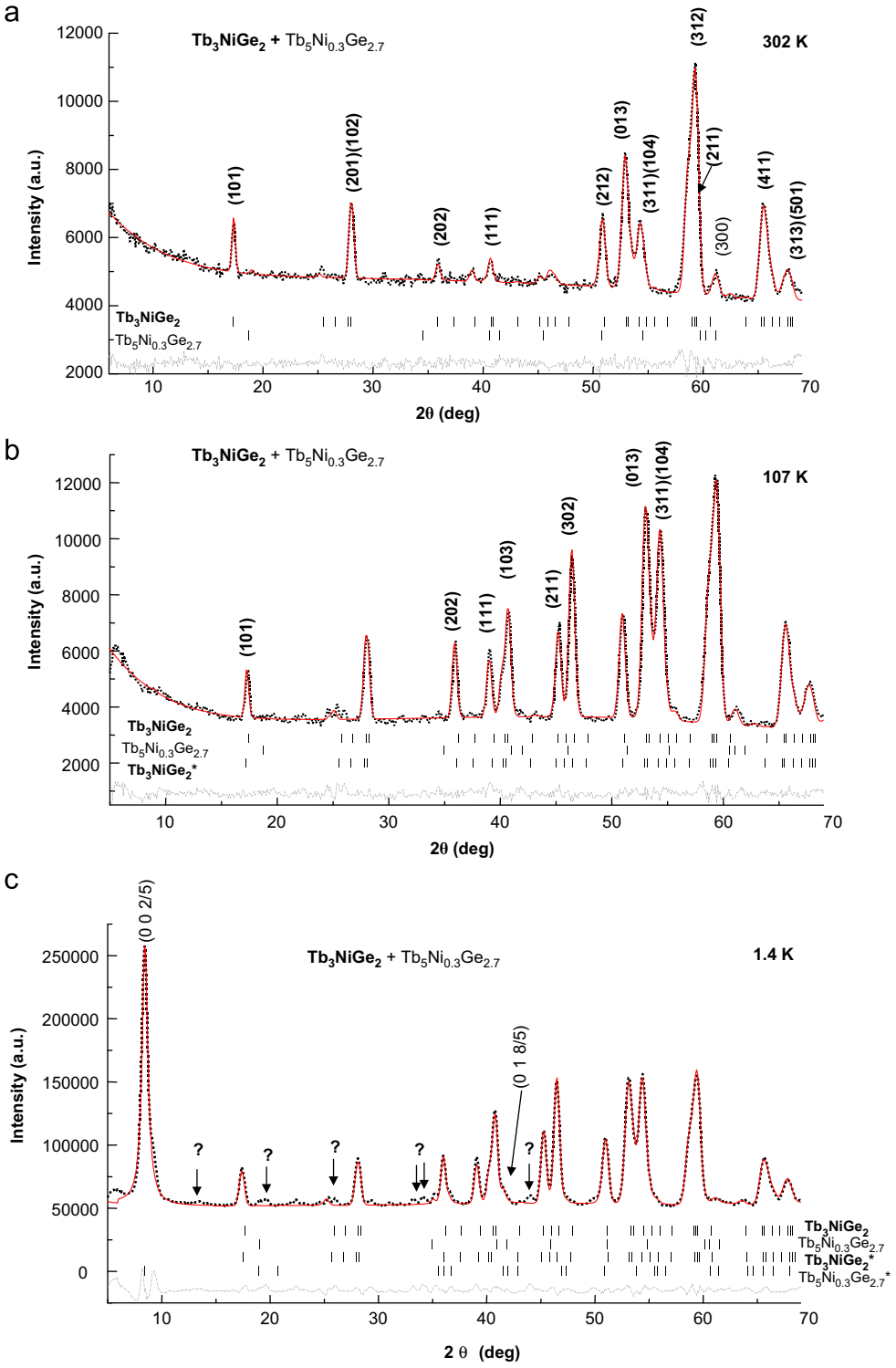

Fig. 4. Neutron diffraction patterns of the 'Tb_3NiGe_2' sample (a) recorded at a wavelength of 0.252 nm and at 302 K (paramagnetic state), (b) at 107 K (ferromagnetic state of La_3NiGe_2-type Tb_3NiGe_2 and paramagnetic state of Mn_5Si_3-type $Tb_5Ni_{0.3}Ge_{2.7}$) and (c) at 2 K (ferromagnetic state of Tb_3NiGe_2 and antiferromagnetic state of $Tb_5Ni_{0.3}Ge_{2.7}$). Strong magnetic reflections are shown in (b) and (c). *Magnetic part of the corresponding compound.

reveals that the additional magnetic reflections of $Tb_5Ni_{0.3}Ge_{2.7}$ correspond to the part of the unit cell with propagation vectors $K=[0, 0, \pm K_c]$ and flat spiral antiferromagnetic ordering (Fig. 4c).

Thermal variation of the Tb magnetic moments in the 6*g* and 4*d* sites and K_c are given in Fig. 5b and c. The terbium magnetic moment at the 6*g* site is smaller than the one at 4*c* from 89 K down to 1.4 K. At 2 and 10 K the K_c value indicates the magnetic unit cell $a \times a \times 5c$. From 10 K up to 89 K the K_c increases from 2/5 up to 0.4205(5).

The neutron diffraction patterns of the 'Tb_3NiGe_2' sample contain a small incommensurate unindexed reflection with 2θ of 13°, 19°, 26°, 33° and 44° at 1.4 K that may belong to the small magnetic component of Tb_3NiGe_2, $Tb_5Ni_{0.3}Ge_{2.7}$ or unindexed magnetic impurity phases.

We may conclude from the present experimental data that the presence of Ni atoms decreases the magnetic unit cell from $a \times a \times 40c$ of Tb_5Ge_3 down to $a \times a \times 5c$ of $Tb_5Ni_{0.3}Ge_{2.7}$ and both

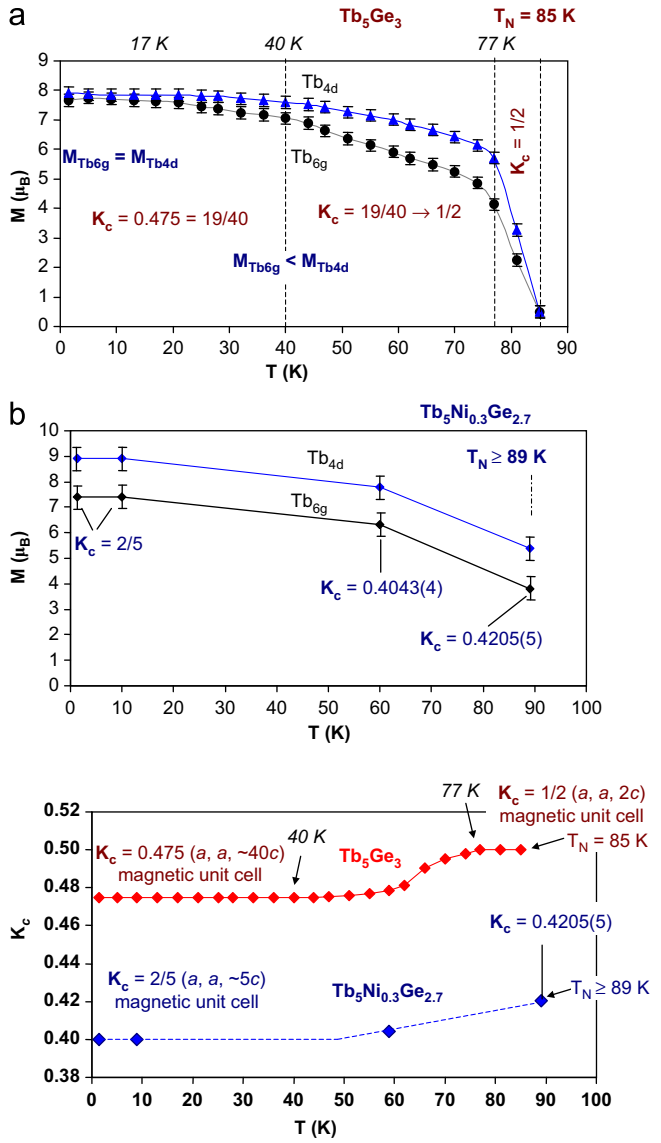

Fig. 5. Thermal evolution of Tb magnetic moment at 6g and 4*d* sites of (a) Tb_5Ge_3 and (b) $Tb_5Ni_{0.3}Ge_{2.7}$ and (c) K_c component of wave vector of Tb_5Ge_3 and $Tb_5Ni_{0.3}Ge_{2.7}$.

Table 3
Crystallographic and magnetic parameters of Mn_5Si_3-type Tb_5Ge_3 and $Tb_5Ni_{0.3}Ge_{2.7}$ compounds at different temperatures: cell parameter, M_{Tbj} the magnitude of Tb magnetic moment at the 6g and 4*d* sites and magnitude of K_c component of $K_c=[0, 0, \pm K_c]$ wave vector. Reliability factors are R_F for crystal structure and R_F^m for magnetic structure.

T (K)	Unit cell data (nm)	R_F (%)	Atom	M_{Tbj} (μ_B)	K_c	R_F^m (%)
	Tb_5Ge_3					
300[a]	a=0.84956(6)	4.1				
	c=0.63861(4)					
295	a=0.8491(4)	6.2				
	c=0.6382(4)					
81	a=0.8476(3)	9.7	**Tb_{6g}**	2.2(2)	1/2	12.5
	c=0.6363(3)		**Tb_{4d}**	3.3(2)		
1.5	a=0.8469(4)	6.7	**Tb_{6g}**	7.8(1)	0.475(2)=19/40	5.4
	c=0.6365(4)		**Tb_{4d}**	7.8(1)		
	$Tb_5Ni_{0.3}Ge_{2.7}$					
300[a]	a=0.8472(3)	2.3				
	c=0.6348(2)					
302	a=0.8502(4)					
	c=0.6338(6) nm	6.5				
89	a=0.8479(5)	6.8	**Tb_{6g}**	3.8(3)	0.4205(5)	6.3
	c=0.6331(7)		**Tb_{4d}**	5.4(4)		
60	a=0.8482(8)	6.4	**Tb_{6g}**	6.3(3)	0.4043(4)	2.7
	c=0.6332(8)		**Tb_{4d}**	7.8(4)		
10	a=0.8485(8)	6.8	**Tb_{6g}**	7.4(3)	0.4005(3)	2.4
	c=0.6343(9)		**Tb_{4d}**	8.9(5)		
			Tb_{4d}			
1.4	a=0.8483(7)	7.0	**Tb_{6g}**	7.4(3)	0.4002(3) ≈ 2/5	3.2
	c=0.6341(7)		**Tb_{4d}**	8.9(5)		

Table 4
Atomic positions of the 4*c* sites of space group *Pnma* (retained by Tb_3NiGe_2 compound) with the corresponding symmetry operators and subgroups.

N	*x*/*a*	*y*/*b*	*z*/*c*	Symmetry operation	Point subgroup of 4*c* site			
					D_2	C_{2v}	C_{2h}	C_{2h}
1	x	1/4	z	{**1**, $\mathbf{m}_y$/[0 1/2 0]}	**1**	**1**	**1**	**1**
2	1/2−x	3/4	1/2+z	{$\mathbf{2}_z$/[1/2 0 1/2], $\mathbf{m}_x$/[1/2 1/2 1/2]}	$\mathbf{2}_z$	$\mathbf{m}_x$	$\mathbf{m}_x$	$\mathbf{2}_z$
3	1/2+x	1/4	1/2−z	{$\mathbf{m}_z$/[1/2 0 1/2], $\mathbf{2}_x$/[1/2 1/2 1/2]}	$\mathbf{2}_x$	$\mathbf{m}_z$	$\mathbf{2}_x$	$\mathbf{m}_z$
4	−x	3/4	−z	{$\bar{\mathbf{1}}$, $\mathbf{2}_y$/[0 1/2 0]}	$\mathbf{2}_y$	$\mathbf{2}_y$	$\bar{\mathbf{1}}$	$\bar{\mathbf{1}}$

Tb_5Ge_3 and $Tb_5Ni_{0.3}Ge_{2.7}$ have antiferromagnetic flat spiral magnetic ordering. The magnetic moments of Tb atoms in Tb_5Ge_3 and $Tb_5Ni_{0.3}Ge_{2.7}$ are (see Tables 2 and 3)

$$M_{Tbj} = M_{Tbj}\,\mathbf{i}\cos(2\pi K_c[n+Z_{Tbji}]) + \mathbf{j}\sin(2\pi K_c[n+Z_{Tbji}]),$$

where n=0, 1, 2, … is the number of unit cells along the *c* axis; **i** and **j** are orthonormal vectors in the *ab* plane; **i** coincides with the *a* axis of unit cell.

3.3. *Magnetic structure of La_3NiGe_2-type Tb_3NiGe_2.*

The La_3NiGe_2-type Tb_3NiGe_2 compound (space group *Pnma*, point group $\mathbf{D}_{2h}$) consists of 4*c* sites of terbium, nickel and germanium (Table 2). The 4*c* site atomic positions and symmetry operators of the corresponding terbium and nickel sublattices are given in Table 4. The subgroups of the $\mathbf{D}_{2h}$ point group that correspond to the 4*c* site of *Pnma* are $\mathbf{D}_2$, $\mathbf{C}_{2h}$ and $\mathbf{C}_{2v}$ point groups. These 'colorless' point groups and 'black–white' $\mathbf{D}_2'$, $\mathbf{C}_{2h}'$ and $\mathbf{C}_{2v}'$ magnetic point groups [7,8] were used for analysis of neutron diffraction data.

At 135 K the set of commensurate magnetic reflections reveals the magnetic ordering of Tb_3NiGe_2. The collinear ferrimagnetic structure with antiparallel alignment of rare earth and nickel magnetic moments along the *b* axis is found to give the best agreement with experimental data (Figs. 4 and 6). The following magnetic point group corresponds to *b*-collinear ordering: $\mathbf{D}_2'=\{\mathbf{1}, 1'\times\mathbf{2}_x, \mathbf{2}_y, 1'\times\mathbf{2}_z\}$, $\mathbf{C}_{2v}=\{\mathbf{1}, \mathbf{m}_x, \mathbf{2}_y, \mathbf{m}_z\}$, $\mathbf{C}_{2h}'=\{\mathbf{1}, \mathbf{m}_x, 1'\times\mathbf{2}_x, 1'\bar{\times}\mathbf{1}\}$ or $\mathbf{C}_{2h}'=\{\mathbf{1}, \mathbf{m}_z, 1'\times\mathbf{2}_z, 1'\bar{\times}\mathbf{1}\}$. The Tb magnetic moment increases with decreasing temperature, whereas the Ni magnetic moment is almost constant at about 0.7 μ_B in this temperature range below 135 K (Fig. 7). At 1.4 K the terbium magnetic moments reach values of 7.37 μ_B (Fig. 7 and Table 5). The magnitude of Ni moment is close to the 0.62 μ_B of pure Ni, whereas the magnetic moment of Tb is somewhat less than the 9 μ_B value expected for free ion Tb^{3+} [6].

As reported recently, the known magnetic structure of La_3NiGe_2-type Pr_3CoGe_2 and Nd_3CoGe_2 shows an *ac* plane AF–F structure corresponding to $\mathbf{D}_2'=\{\mathbf{1}, \mathbf{2}_x, 1'\times\mathbf{2}_y, 1'\times\mathbf{2}_z\}$, $\mathbf{C}_{2v}'=\{\mathbf{1}, \mathbf{m}_x', \mathbf{2}_y', \mathbf{m}_z\}$, $\mathbf{C}_{2h}'=\{\mathbf{1}, 1'\times\mathbf{m}_x, \mathbf{2}_x, 1'\bar{\times}\mathbf{1}\}$ or $\mathbf{C}_{2h}'=\{\mathbf{1}, \mathbf{m}_z, 1'\times\mathbf{2}_z,$

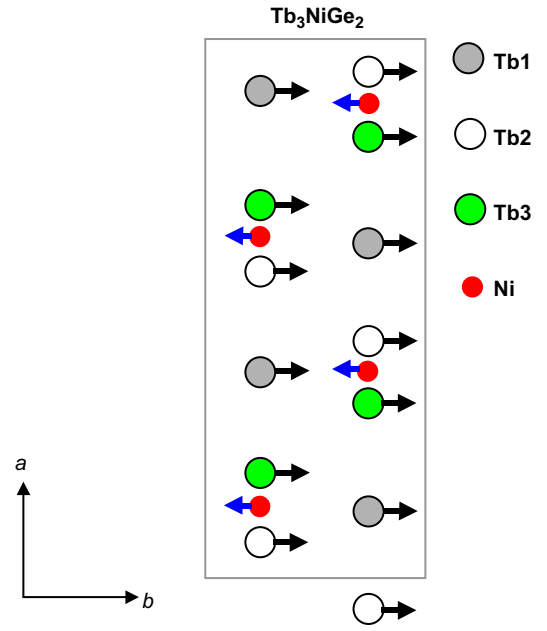

Fig. 6. Image of collinear ferrimagnetic structure of La_3NiGe_2-type Tb_3NiGe_2 below ~135 K.

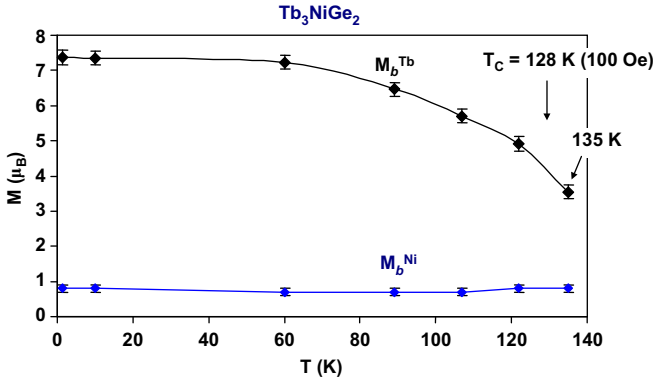

Fig. 7. Thermal evolution of Tb and Ni magnetic moments in Tb_3NiGe_2.

$1' \bar{\times} \mathbf{1}\}$ magnetic point groups [9]. The last $\mathbf{C}_{2h}{}' = \{\mathbf{1}, \mathbf{m}_z, 1' \times \mathbf{2}_z, 1' \bar{\times} \mathbf{1}\}$ magnetic point group designs both the *ac* plane ordering of {Pr, Nd}$_3$CoGe$_2$ and the *b*-collinear one of Tb_3NiGe_2.

4. Conclusion

The ferrimagnetic nature of La_3NiGe_2-type Tb_3NiGe_2 is evident both from both magnetization and neutron diffraction studies. Analysis of the powder neutron diffraction results has shown that the Tb_3NiGe_2 compound exhibits a commensurate *b*-collinear ferrimagnetic ordering with $\mathbf{C}_{2h}{}' = \{\mathbf{1}, \mathbf{m}_z, 1' \times \mathbf{2}_z, 1' \bar{\times} \mathbf{1}\}$ magnetic point group. The investigation of Ni for Ge substitution in the $Tb_5Ni_xGe_{3-x}$ (x=0–0.3) system demonstrates that a similar flat spiral magnetic order is observed in both compounds but the presence of Ni atoms decreases the magnetic unit cell of the flat spiral structure from $a \times a \times 40c$ of Tb_5Ge_3 (below 40 K) down to $a \times a \times 5c$ of $Tb_5Ni_{0.3}Ge_{2.7}$ (below ~10 K).

Table 5
Crystallographic and magnetic parameters of La_3NiGe_2-type Tb_3NiGe_2 at different temperatures: cell parameters, M_b^{Tb} and M_b^{Ni} the magnitude of Tb and Ni magnetic moments along the *b* axis, respectively. Reliability factors are: R_F for crystal structure and R_F^m for magnetic structure.

T (K)	a (nm)	b (nm)	c (nm)	R_F (%)	M_b^{Tb} (μ_B)	M_b^{Ni} (μ_B)	R_F^m (%)
300[a-]	1.1403(1)	0.41793(4)	1.1248(1)	2.5			
302	1.1405(2)	0.41906(9)	1.1244(2)	6.5			
297	1.1405(2)	0.41915(9)	1.1244(3)	8.1			
270	1.1405(2)	0.41903(9)	1.1242(2)	7.9			
238	1.1401(2)	0.41887(9)	1.1238(2)	7.9			
208	1.1396(2)	0.41877(9)	1.1235(2)	7.8			
183	1.1393(3)	0.4187(1)	1.1230(2)	7.9			
167	1.1394(3)	0.4187(1)	1.1232(3)	7.6			
157	1.1390(3)	0.4186(1)	1.1231(3)	7.5			
154	1.1392(2)	0.4185(1)	1.1228(3)	7.7			
149	1.1391(3)	0.4184(1)	1.1226(3)	7.9			
144	1.1392(3)	0.4185(1)	1.1225(3)	7.9			
142	1.1396(3)	0.4185(1)	1.1226(3)	6.2			
135	1.1394(2)	0.41795(8)	1.1219(2)	6.0	3.55(7)	−0.8(1)	8.7
122	1.1396(2)	0.41767(6)	1.1218(2)	5.8	4.91(7)	−0.8(1)	7.5
107	1.1394(2)	0.41744(6)	1.1216(2)	5.3	5.70(7)	−0.7(1)	6.6
89	1.1394(2)	0.41736(6)	1.1216(2)	4.7	6.46(8)	−0.7(1)	5.3
60	1.1397(2)	0.41740(6)	1.1218(2)	3.8	7.23(8)	−0.7(1)	4.3
10	1.1410(1)	0.41775(6)	1.1230(1)	3.6	7.35(8)	−0.8(1)	4.3
1.4	1.1410(2)	0.41776(7)	1.1229(2)	3.7	7.37(9)	−0.8(1)	4.1

[a-] X-ray data.

Acknowledgments

The Institute Laue Langevin is warmly acknowledged for the use of the neutron diffraction beam. This work was supported by the Russian Fund for Basic Research through Project no. 12-03-00428-a.

References

[1] Pearson's Handbook of Crystallographic Data for Intermetallic Phases, American Society for Metals, Metals Park, OH (1985) 1–3.
[2] P. Schobinger-Papamantelos, Journal of Magnetism and Magnetic Materials 28 (1982) 97.
[3] F. Izumi, in: R.A. Young (Ed.), The Rietveld Method, Oxford University Press, Oxford, 1993. (Chapter 13).
[4] www.ill.eu, Yellow Book.
[5] J. Rodriguez-Carvajal, Physica B—Condensed Matter 192 (1993) 55–69.
[6] S. Legvold, Rare Earth Metals and Alloys, in: E.P. Wohlfarth (Ed.), Ferromagnetic Materials, North-Holland Publishing Company, Amsterdam, 1980, pp. 183–295.
[7] P.S. Kireev, Introduction to Group Theory and its Application in Solid State Physics, High School, Moscow, 1979 in Russian.
[8] C.J. Bradley, A.P. Cracknell, The Mathematical Theory of Symmetry in Solids, Clarendon, Oxford, 1972.
[9] P. Manfrinetti, A.V. Morozkin, O. Isnard, F. Wrubl, Yu. Mozharivskyj, V. Svitlyk, Intermetallics 19 (2011) 321–326.